TURBULENT VELOCITY AND TEMPERATURE FIELDS IN THE NONISOTHERMAL WAKE BEHIND AN ELONGATED BODY OF REVOLUTION

Yu. M. Dmitrenko, V. L. Zhdanov,
and B. A. Kolovandin

UDC 532.517.4:532.582.33

Results of an experimental investigation of turbulent velocity and temperature fields in the wave behind an axisymmetric body are presented.

For many years the attention of researchers to the study of axisymmetric wakes behind bodies of different shape has not attenuated. One of the fundamental factors stimulating this interest is the demand for effective methods of analyzing the turbulence characteristics that would permit predicting the dynamics of the turbulence parameters of isothermal and nonisothermal shear coflows. Without detailed experiments on "model" flows it is impossible to solve this problem. At this time the velocity field characteristics have been investigated most completely. The influence of the shape of the model being streamlined on the turbulent flow structure [1-4], which is that the wake parameters achieve self-similar asymptotic dependences at different distances for substantially different bodies while the proportionality factors of these dependences are functions of the shape of these models has here been clarified. As regards the papers devoted to the thermal wake, in the literature there are only shear flow characteristics behind a disc [5], sphere [6-8], and for a heated circular cojet [9]. Most informative in this respect is [6]. It is there shown that starting with the relative distance $x_1/d = 80$, the thermal wake develops self-similarly as does the velocity wake, but in contrast to other kinds of jet and wake nonisothermal flows in this domain, the velocity and temperature profiles are of identical width.

The present paper has the task, first, of clarifying which of the dependences of the nonisothermal shear flow characteristics behind axisymmetric bodies are universal and which are determined by the body shape; second, of estimating the influence of the dynamic flow parameters on the development of the thermal wake.

The experiment was performed in a wind tunnel with 0.5 × 0.5 × 3.75 m closed working section which is described in detail in [4]. The model, an ellipsoid of revolution with d = 30 mm middle section diameter and 6:1 ratio of the axes, was suspended by eight 0.2-mm-diameter wire bracings. The thermal wake was produced by injection of a heated air jet through a 3-mm-diameter orifice in the stern area of the model. Two modes were investigated: for 14.3 and 26.9 m/sec jet rates of expulsion (modes I and II, respectively). The free stream velocity was constant U_∞ = 10 m/sec in both cases. The initial temperature difference $\Delta T_j = T_0 - T_\infty$ at the distance $x_1/d = 0.1$ was 60°C for both modes. For such a heating level the temperature exerted no influence on the wake velocity field and was transferred as a passive impurity, as was confirmed by the agreement between the cold and heated jet velocity profiles. The flow temperature in the tunnel was maintained automatically at 24±0.1°C. The flow behind the model was a wake, i.e., had a negative excess momemtum for modes I and II.

The turbulence characteristics were measured by a thermonanemometer unit of the firm "DISA" (constant temperature thermoanemometers 55M01 and 55D01, filtration module 55D26, effective value voltmeter 55D35, linearizers 55D10). Specialized devices developed in the Special Design Bureau of the Institute of Heat and Mass Transfer of the Belorussian Academy of Sciences were also used (add and subtract modules, module to compensate the thermal inertia of the sensor wire, integrator, differentiator). The velocity fluctuations were measured by 55P01 and 55P51 probes of the firm "DISA" by a standard methodology. The probes were calibrated in an unperturbed flow by means of a Pitot–Prandtl tube at the beginning of each experiment. The mean temperature was determined by a differential Chromel–constantan thermocouple fabricated from 0.2-mm-diameter wire by using a V7-21 digital voltmeter with ±1-μV

A. V. Lykov Institute of Heat and Mass Transfer, Academy of Sciences of the Belorussian SSR, Minsk. Translated from Inzhenerno-Fizicheskii Zhurnal, Vol. 50, No. 1, pp. 14-22, January, 1986. Original article submitted November 6, 1984.

0022-0841/86/5001-0009$12.50

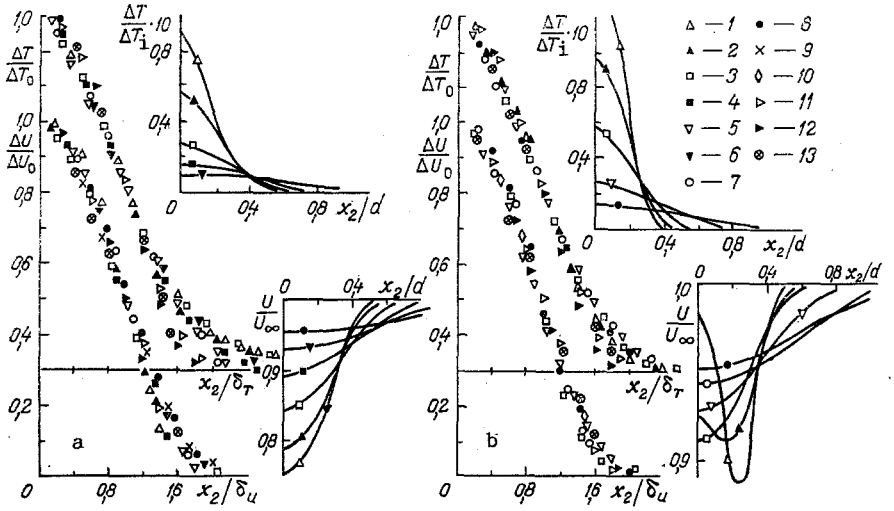

Fig. 1. Distribution of the mean velocity and temperature along the radius in different wake sections for regimes I (a) and II (b): 1) $x_1/d = 3$; 2) 5; 3) 10; 4) 20; 5) 30; 6) 40; 7) 50; 8) 70; 9) data [10]; 10) [11]; 11) [6]; 12) [5]; 13) [9].

error (which corresponds to ±0.016°C). One of the junctions was placed in the free stream and the other in the wake. The temperature fluctuations were measured by probes 55P31 of the firm "DISA" (1-μm-diameter wire, 0.4 mm in length) and a 55D01 aneometer operating in the d/c mode. For a selected 0.7-mA measuring current, the probe sensitivity to velocity fluctuations was negligible as compared with the sensitivity to temperature fluctuations. The band of reproducible frequencies was broadened by using a module to compensate the thermal inertia of the wire (to approximately 20 kHz for a 10-m/sec velocity). The velocity and temperature field microscales λ_u and λ_θ were estimated in conformity with the Taylor hypothesis

$$\lambda_u = U\,[\overline{u_1^2}/\overline{(\partial u_1/\partial t)^2}]^{1/2}, \quad \lambda_\theta = U\,[\overline{\theta^2}/\overline{(\partial\theta/\partial t)^2}]^{1/2}. \tag{1}$$

Derivatives of the signals were obtained by using a broadband analog differentiator (with not more than 0.5% deviation of the characteristics from the ideal in a 0.1-Hz–40-kHz range). The measured values of the turbulent fluctuations and microscales were corrected for the instrument noise and background turbulence of the wind tunnel by the method described in [4].

Results of the experiments are represented in Figs. 1-5 in dimensionless form with the velocity and temperature characteristics compared for each mode. Normalization was performed to the appropriate characteristic length, velocity, and temperature scales (d, U_∞, ΔT_i) in analyzing the evolution of the characteristics along the wake axis, and to the values on the axis of symmetry, denoted by the subscript "0" and corresponding to the wake half-width (for the transverse coordinate) governed by the profiles of the mean and fluctuating velocity and temperature δ_U, δ_1, δ_T, δ_θ, for the estimate of the similarity of the radial profiles at different distances from the model. The half width along any characteristic was taken equal to the distance at which its value is half that on the wake axis of symmetry. Such normalization is convenient even for a comparison with the data of other authors although the influence of the model shape is hidden here. It is more correct to execute the comparison with the drag coefficient C_x of each model taken into account [2]; however, not all authors present this coefficient.

As follows from Fig. 1, the jet exerts noticeable influence on the nature of the flow around the body and on the structure of the near-wake domains. At high jet velocities (Fig. 1b), the mean velocity profile in the wake has a complex shape with "jet" and "wake" sections up to the relative distances $x_1/d = 7$. Similarity in the mean velocity profiles is observed for $x_1/d > 5$ and $x_1/d > 10$, respectively, for modes I and II. The average velocity profiles are identical for both modes and agree with those obtained in other axisymmetric flows (in particular, in wakes behind an ellipsoid of revolution [10], a streamlined body [11], a sphere [1], an elongated cone [5], and in a cojet [9]). An increase in the velocity of jet escape results in a rise in the excess temperature on the axis and a diminution in the width

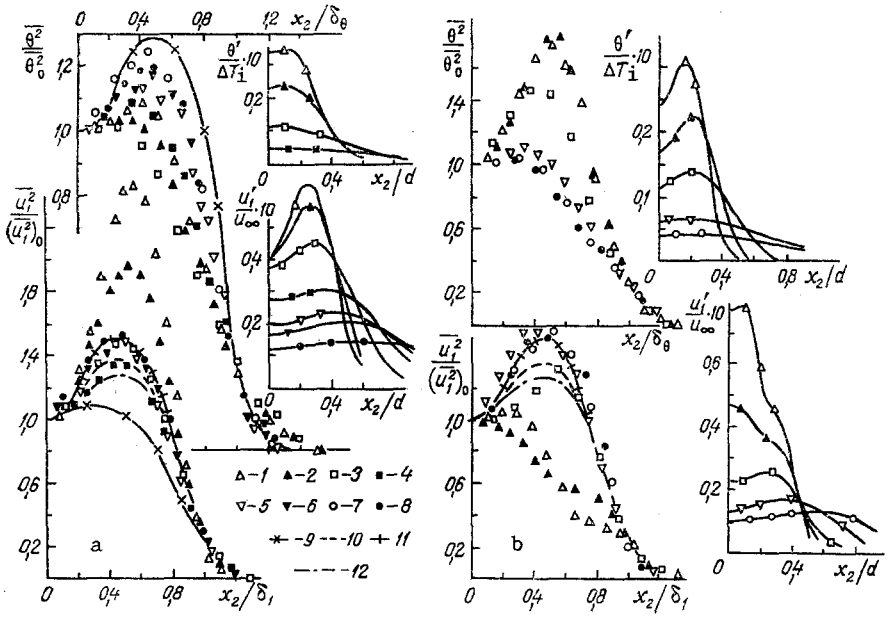

Fig. 2. Radial velocity and temperature fluctuation profiles for modes I (a) and II (b) at different wake sections: x_1/d = 3; 2) 5; 3) 10; 4) 20; 5) 30; 6) 40; 7) 50; 8) 70; 9) data [6]; 10) [11]; 11) [10]; 12) [9].

of the thermal wake. Self-similar excess temperature profiles are also independent of the flow mode and are close to the profiles measured in nonisothermal wakes behind a disc [5], sphere [6], in a round heated jet in a coflow [9], with the exception of the domain near the wake boundary. Comparing the data we present for this domain and the results in [5, 6, 9], the deduction can be made that the excess temperature turns out to be sensitive to a change in the flow initial conditions as contrasted with the mean velocity. Both the stratification of the $\Delta T/\Delta T_0$ profiles for mode I for $x_1/d \leqslant 10$ and the diminution in the self-similar profile width $\Delta T/\Delta T_0$ during passage from a good streamlined model (the present paper) to models characterized by high values of the coefficients C_X [5, 6] indicate this.

Analysis of the distributed velocity and temperature fluctuations along the wake radius (Fig. 2) results in a number of conclusions some of which (referring to the velocity field characteristics) confirm facts already known, namely, growth of the sensitivity of the turbulence characteristics (moments) to wake structure with the increase in their order, and others, associated with the temperature fluctuations, are new.

The self-similar velocity fluctuation profiles (their similarity for modes I and II was observed from the distance x_1/d = 30), which are identical for both models are in good agreement with analogous ones measured in [2, 4, 10] but differ from the profile in the wake behind a sphere [6]. Therefore, the velocity fluctuations at large distances from the body retain "memory" only about substantial differences in the initial conditions (that appear, in particular, in differences in the drag coefficients of comparable bodies). Bodies that are close in shape [2, 4, 10] yield a similar fluctuation distribution.

To a large extent temperature fluctuations are subject to the influence of initial conditions as compared to the velocity fluctuations as is reflected in the different shape of the average profiles for modes I and II obtained at distances $x_1/d > 30$. Let us emphasize that degeneration of the fluctuations occurs for this wake domain according to a power law with exponent −0.9 for both modes (Fig. 3). Since the thermal wake investigated has still not reached the domain of self-similar development, it is premature to make a deduction about the qualitative and quantitative correspondence between the temperature fluctuation profiles and the self-similar profile in the wake behind a sphere [6]. Let us recall that the data of [6] are closer to those that were obtained for mode I. Ratios between the maximums of the velocity and temperature fluctuations and their values on the axes $(\bar{u}_1^2/(\bar{u}_1^2)_0, \overline{\theta^2}/\overline{\theta^2}_0)$, which equal 1.5 and 1.2 (mode I) have still not arrived at the limit value. However, the probability is low that we will obtain $\overline{\theta^2}/\overline{\theta}_0^2 > \bar{u}_1^2/(\bar{u}_1^2)_0$, as was reported in [6, 11]. It is known that a change in the turbulence characteristics along the axis is described by the following asymptotic dependences in the self-similar domain of axisymmetric wake development

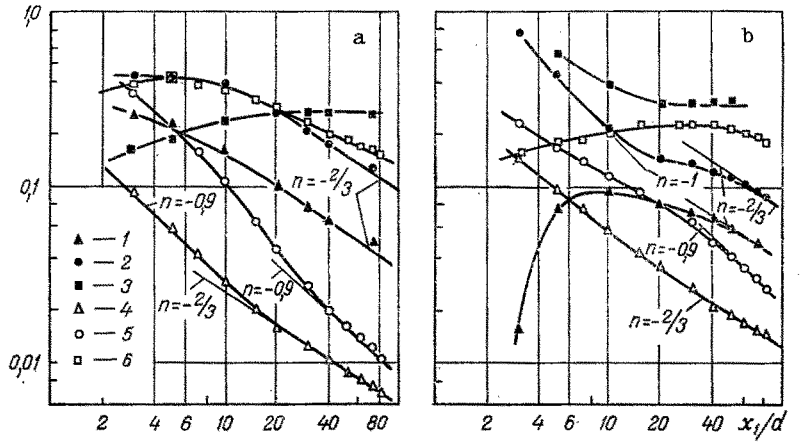

Fig. 3. Dependence of the mean and fluctuating magnitudes of the velocity and temperature on the longitudinal coordinate for modes I (a) and II (b): *1* — $\Delta U_0/U_\infty$; *2* — $((u_1')_0/U_\infty)\cdot 10$; *3* — $(u_1')_0/\Delta U_0$; *4* — $\Delta T_0/\Delta T_i$; *5* — $(\theta_0'/\Delta T_i)\cdot 10$; *6* — $\theta_0'/\Delta T_0$.

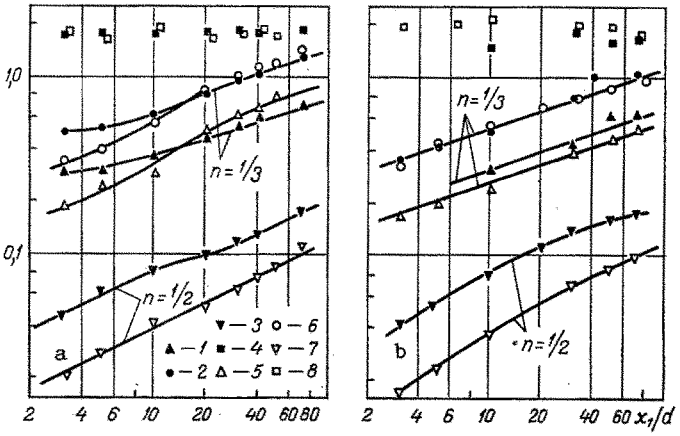

Fig. 4. Dependence of the wake width and velocity and temperature field microscales on the longitudinal coordinate for modes I (a) and II (b): *1* — δ_U/d; *2* — δ_1/d; *3* — λ_u; *4* — δ_U/δ_1; *5* — δ_T/d; *6* — δ_θ/d; *7* — λ_θ; *8* — δ_T/δ_θ .

$$(u_1')_0/U_\infty \sim \Delta U_0/U_\infty = C_u (x_1/d)^{-2/3},\ \theta_0'/\Delta T_i \sim \Delta T_0/\Delta T_i = C_T (x_1/d)^{-2/3},$$
$$\delta_U \sim \delta_T \sim \delta_1 \sim \delta_\theta = C_\delta (x_1/d)^{1/3}. \qquad (2)$$

The proportionality factors (C_U, C_T, C_δ) and the distances at which the flow starts to become self-similar are functions of the body shape. In particular, the dependences (2) for the velocity field are satisfied in the wake behind a heated sphere [6] for $x_1/d = 50$, while for $x_1/d = 80$ for the temperature field. In the case of an ellipsoid of revolution [4], development of the velocity wake in conformity with the dependences (2) is observed for $x_1/d = 20$. Self-similarity of the velocity field for mode I starts with precisely this distance while the dynamic flow parameters followed the power laws (2) from 40 calibers for mode II (Fig. 3).

Only the excess temperature reaches the self-similar domain in the thermal wake. For mode I this domain starts with the distance $x_1/d > 20$ while it starts with $x_1/d = 10$ for mode II, i.e., the nature of the change in excess temperature as a function of the jet ejection velocity is directly opposite to that observed for the velocity defect.

It is interesting to compare the results obtained (Fig. 3) with those presented in [7], where the thermal wake behind a sphere was also produced by injection of a heated fluid in

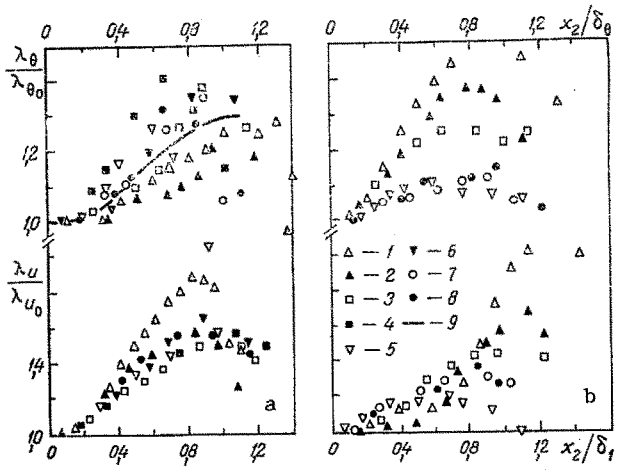

Fig. 5. Radial velocity and temperature field microscale profiles for modes I (a) and II (b) in different wake sections: 1) $x_1/d = 3$; 2) 5; 3) 10; 4) 20; 5) 30; 6) 40; 7) 50; 8) 70; 9) data [6].

in the reverse current zone. The exponents in the laws of the decrease in the quantities ΔT_0 and θ_0^2 equaled −0.8 in the domain $x_1/d \leqslant 50$ in [7], and −0.85 for the quantity u_1^2/U_∞ up to the distance $x_1/d = 100$. Close values are also observed for both flow modes investigated. For the former, degeneration of the excess temperature and the temperature fluctuations in the near wake is described by a power law with exponent −0.9 for the latter they equal −0.8 and −0.6, respectively. The velocity fluctuations vary according to a law with exponent −1. Therefore, despite the substantial differences in the experiment conditions, the rates of degeneration of the turbulence characteristics in the transition domain turn out to be close. Moreover, comparison with the results in [6] permits making a deduction about the shift in the self-similarity domain for the velocity field at large distances from the body in the presence of a jet flow section in the wake.

Analysis of the velocity and temperature field fluctuation characteristics in the wake of an ellipsoid for two values of the jet velocity showed that the temperature fluctuations decrease as the velocity fluctuations grow, and conversely. Such behavior was observed in both the near and the far wake.

The self-similarity domain is characterized by constancy of the ratios $(u_1')_0/\Delta U_0$ and $\theta_0'/\Delta T_0$ on the wake axis. For mode I the ratio $(u_1')_0/\Delta U_0 = 0.26$, while for mode II it is 0.21. It equals 0.26 in the wake behind a well-streamlined body while it is 0.69 [6] and 0.6 [8] in the wake behind a sphere. Therefore, for well-streamlined bodies the self-similar values $(u_1')/\Delta U_0$ are in agreement within the limits of experimental error and almost three times lower than in the case of poorly streamlined bodies. Although the ratio $\theta_0'/\Delta T_0$ did not reach the asymptotic value in the thermal wake domain investigated because of the absence of self-similarity, it can be asserted that it does not exceed 0.2. Since an analogous quantity equals 0.76 in experiments [6], and 0.38 in [7], it is natural to assume that the characteristics of a self-similar thermal axisyymmetric wake depend on the shape and features of the flow around the body exactly as strongly as for the dynamic wake.

The dependences describing the change in scale of the velocity and thermal wakes (the halfwidths of the mean and fluctuating characteristic profiles, the microscales) are represented in Fig. 4. All the characteristics under consideration (δ_U, δ_T, δ_1, δ_θ, λ_u, λ_θ) emerge on the self-similar asymptotic laws (2), however the distances at which these laws start to be satisfied depend on the jet ejection velocity. The beginning of the self-similar section corresponds to the distance $x_1/d = 20$ for a lower ejection velocity for the quantities δ_U, δ_T, δ_1, δ_θ while $x_1/d = 3$ for higher velocities. The width of the thermal wake for the first mode is less than the width of the velocity wake to the distance $x_1/d = 20$, while they later are different. For the second mode the velocity and temperature fluctuation profiles are practically identical while the excess temperature profiles are narrower than the mean velocity profiles in the whole distance band. The relationships obtained for the thermal and velocity wake widths agree with the results in [6], and are visibly universal for axisymmetric bodies.

TABLE 1. Microscale Correction Factors for the Probe Finite Resolution

x_1/d		3	5	10	20	30	40	50	70
K_u	Mode I	0,84	0,87	0,89	0,925	0,95	0,96	0,97	0,985
	Mode II	0,78	0,85	0,88	0,925	0,95	0,96	0,97	0,985
K_θ	Mode I	0,51	0,55	0,61	0,65	0,69	0,72	0,73	0,74
	Mode II	0,59	0,61	0,67	0,69	0,71	0,72	0,73	0,75

An interesting feature appears in comparing the width of the fluctuating profiles with the velocity and excess temperature profiles. The ratios δ_1/δ_U, δ_θ/δ_T were constant and equal to 1.2 for both modes in the whole distance interval despite the absence of self-similarity in the thermal wake.

As our investigations showed, the structure of the thermal wake was of a finer scale as compared with the velocity field structure, and the difference between the temperature and velocity microscales increased with the rise in the jet velocity.

The microscale distribution along the wake radius is represented in Fig. 5. In contrast to the other wake characteristics, a matched change in the quantities λ_u and λ_θ is observed for both modes. The self-similar profile of the temperature microscale for mode I corresponded qualitatively to that obtained in the wake behind a sphere [6]. Growth of the jet ejection velocity from the model resulted in the microscale distribution along the radius becoming more homogeneous. This occurred for the temperature microscale at greater distances from the model ($x_1/d > 10$), which indicates the greater sensitivity of the temperature field to the initial conditions.

It should be noted that the microscales presented in Figs. 4 and 5 received corrections of the directly measured values by the finite resolution of the probe wires $\lambda_u = \lambda_u^* K_u$, $\lambda_\theta = \lambda_\theta^* K_\theta$, λ_u^* and λ_θ^* are the measured values. Rated dependences presented in [12, 13] were used for corrections. The correction factors K_u and K_θ for the velocity and temperature microscales are presented in the table.

The data in the table show that the temperature field microscale correction was significant in all sections where the measurements were performed while it became inessential for the velocity microscale starting with $x_1/d = 30$.

The experimental investigations executed, as well as the analysis of data about axisymmetric wakes available in the literature permits making the deduction that the temperature field characteristics retain a "memory" about the initial conditions considerably longer than do the corresponding velocity field characteristics. Complete independence of the thermal wake development in a velocity field was observed here (with the exception of the microscales).

NOTATION

U, axial velocity component; $\Delta U = U - U_\infty$, defect in the mean velocity: u_1, logitudinal velocity fluctuation; $\Delta T = T - T_\infty$, excess temperature; T, mean temperature; $\Delta T_i = T_0 - T_\infty$, initial temperature difference on the wake axis at the distance 0.1d; θ, temperature fluctuation; d, diameter of the middle section of the model; x_1, x_2, longitudinal and transverse coordinates; δ_U, δ_T, δ_1, δ_θ, characteristic transverse dimensions of the wave governed by the profiles U, T, u_1, θ, respectively; λ_u, λ_θ, velocity and temperature field microscales; C_x, model drag coefficient; t, time; C_U, C_T, C_δ, coefficients in the degeneration laws; K_u, K_θ, correction factors to correct the microscales. Indices: upper bar is the time average; 0, parameter value on the wake axis of symmetry; ∞, parameter value in the free stream; ', rms value.

LITERATURE CITED

1. M. S. Uberoi and P. Freymuth, "Turbulent energy balance and spectra of the axisymmetric wake," Phys. Fluids, 13, No. 9, 2205-2210 (1970).
2. V. I. Bukreev, O. F. Vasil'ev, and Yu. M. Lytkin, "On influence of the body shape on self-similar axisymmetric wake characteristics," Dokl. Akad. Nauk SSSR, 207, No. 4, 804-807 (1972).
3. P. M. Bevilaqua and P. S. Lykodis, "Turbulence memory in self-preserving wakes," J. Fluid Mech., 89, Pt. 3, 589-606 (1978).
4. B. A. Kolovandin, N. N. Luchko, Yu. M. Dmitrenko, and V. L. Zhdanov, "Turbulene wake behind an axisymmetric body and its interaction with external turbulence," Preprint No. 10, A. V. Lykov Inst. Heat and Mass Transfer, Beloruss. Acad. Sci., Minsk (1982).

5. H. Reichardt and R. Ermshaus, "Impuls and Warmeubertragung in turbulenten winschatten hinter Rotationskorpern," Int. J. Heat Mass Transfer, 5, 251-265 (1962).
6. P. Freymuth and M. S. Uberoi, "Temperature fluctuations in the turbulent wake behind an optically heated sphere," Phys. Fluids, 16, No. 2, 161-168 (1973).
7. C. H. Gibson, C. C. Chen, and S. C. Lin, "Measurements of turbulent velocity and temperature fluctuations in the wake of a sphere," AIAA J., 6, No. 4, 642-649 (1968).
8. P. Freymuth, "Search for the final period of decay of the axisymmetric turbulent wake," J. Fluid Mech., 68, 812-829 (1985).
9. R. A. Antonia and R. W. Bilger, "The heated round jet in the coflowing stream," AIAA J., 14, No. 11, 1541-1547 (1976).
10. R. Chevret, "Turbulent wake behind a body of revolution," Teor. Osn. Raschetov, No. 3, 164-173 (1968).
11. V. I. Bukreev, V. A. Kostomakha, and Yu. M. Lytkin, "Axisymmetric wake behind a streamlined body," Dinamika Sploshnoi Sred, No. 10, 202-207, Hydrodynamics Inst., Sib. Branch, USSR Acad. Sci., Novosibirsk (1972).
12. J. C. Wynguard, "Spatial resolution of the vorticity meter and other hot-wire arrays," J. Sci. Instrum. (J. Phys. E), Ser. 2, 2, 983-987 (1969).
13. S. Larsen and J. Hojstrup, "Spatial and temporal resolution of a thin-wire resistance thermometer," J. Phys. E. Sci. Instrum., 15, 471-477 (1982).

DATA ON THE STRUCTURE OF THE WALL REGION OF A TURBULENT BOUNDARY LAYER ON AN IMPERMEABLE SURFACE WITH INJECTION

V. T. Kiril'tsev, V. P. Motulevich, and É. D. Sergeivskii

UDC 532.526.4

Methodological aspects are examined in regard to measurements of the components of longitudinal velocity in the wall region of a turbulent boundary layer, and measurements are presented in the case of simultaneous injection and acceleration and turbulence of the main flow.

As is well known, the structure of a flow near the adjacent wall directly determines heat and mass transfer processes and momentum transfer through the turbulent boundary layer. However, for most cases of practical importance, the structure of the flow has been adequately studied only in its external part. The experimental data available for the internal part near the wall is insufficient and often conflicting. This stems from the difficulty of obtaining measurements near the wall (for example, in measurements with a hot-wire anemometer, the difficulty includes allowing for the effect of the proximity of the wall and the high level of turbulence in the wall region on measurements of mean velocity, the spatial resolution of the transducer and the orientation of its tip relative to the wall, and the strict requirement of parallelism of the transducer wire and the wall in measurements of longitudinal-velocity components). Obtaining such measurements is made even more complicated in the presence of mass transfer and acceleration. The velocity field near a permeable wall with injection in a nongradient flow was examined in detail in [1-3], while the same near a nonpermeable wall in the presence of a substantial ($K = (-1.5\text{-}4.0)\cdot 10^{-6}$) pressure gradient was studied in [4].

In experimental study of characteristics of a turbulent boundary layer, the central problem is measuring the skin friction coefficient on the wall C_f. The result obtained in [4] is extremely important in this regard. This study made a comparison of eight common methods of determining C_f: when measuring C_f on a nonpermeable wall in the presence of a pressure gradient, preference should be given to the methods based on the assumption of a linear distribution of the mean component of longitudinal velocity $\bar{U}$ next to the wall. It was found experimentally in [1, 2] that the measurements of $\bar{U}$ next to a porous wall in a nongradient flow with injection agree well with the linear relation $\bar{U} = \text{const}\ y$. In [3], the authors interpreted their test data in the wall region, obtained by the method of flow visualization in a channel in the presence of injection, as agreeing satisfactorily with the

Moscow Energy Institute. Translated from Inzhenerno-Fizicheskii Zhurnal, Vol. 50, No. 1, pp. 22-30, January, 1986. Original article submitted July 30, 1984.

0022-0841/86/5001-0015$12.50